An Interstitial-Electron Model for the Structure of Metals and Alloys II. Electronic Structure of Metals of Groups I—V

Oliver JOHNSON

Research Institute for Catalysis, Hokkaido University, Sapporo

(Received August 9, 1971)

The interstitial-electron model leads to metal structures which are instantaneous pictures of electron distribution written in terms of metal ion core charge M^{n+} (n=valency) and numbers of electrons in octahedral or tetrahedral interstices. On the average there are $\bar{e}$ in all interstices, and the degree of electron localization is small in metals. Decisions as to electron occupancy of interstices are primarily based on considerations of $\bar{e}$ spin and of screening of $\bar{e}$ by ion cores, but electronic heat capacity, Hall coefficient and anisotropy in magnetic susceptibility are of use in making decisions on electron occupancy of interstices. For univalent metals there is little localization of $\bar{e}$ because of the large excess of vacant interstices. This is also true when interstices approach full occupancy by $(\bar{e})_2$ as in M^{4+} and M^{5+}. Among divalent and trivalent metals the preferential occupancy of interstices leads to considerable localization of $\bar{e}$ density for Be, Sc, Y, and Tl. This high degree of localization is a consequence of mutual polarization of ion cores and $\bar{e}$; it accounts for the lattice distortion in these metals and leads to other unusual properties.

The interstitial-electron model for the structure of metals is described in detail in Part I.[1] In order to write such electronic structures for metals, the proper ion core charge (M^{n+}) or valency must be chosen as well as the interstice occupancy by these itinerant or conduction electrons ($\bar{e}$). The itinerant electrons will occupy preferentially the octahedral (oct) or tetrahedral (tet) interstice (I) which offers the maximum screening of its electron from neighboring $\bar{e}$ by positive ion cores and (2) which places $\bar{e}$ of parallel spin farthest away from each other. It turns out for CCP and HCP structures that $\bar{e}$ in adjacent interstices connected by a triangle of ion cores must have opposite spins.

There is a preference for tet occupancy in CCP, no preference in BCC, and a preference which depends on the number of $\bar{e}$ in HCP. For normal HCP lattices there is probably equal oct and tet preference for 1 $\bar{e}/M^{n+}$ since the $\bar{e}$ are widely separated. Since the second $\bar{e}$ in the tet paired interstice is at a short distance ($0.41a$) from the first, at $2\bar{e}$/ion core there will be 1 oct and 1 tet occupied. There will now be tet preference for a second $\bar{e}$ rather than pairing in oct so that at 3 $\bar{e}$ there will be 1 oct and 2 tet occupied. After 3 $\bar{e}$ there is oct preference, again because of the short interstice distance in tet paired interstices. These interstices are shown in Fig. 2 and in Part I. The same preferences for interstice occupancy are expected to hold for the HCP lattice with c/a greater than 1.633 (Zn and Cd).

For HCP lattices with c/a less than 1.633 (Li, Be, Sc) the tet preference is modified by special spin requirements. When all of the bipyramidal interstices (1 BP instead of 2 tet) are occupied, only 1/2 of the oct interstices can be occupied by unpaired electrons. Thus, after 1 1/2 $\bar{e}$, pairing must occur in BP interstices. Between 3 and 4 $\bar{e}$ there is probably pairing in both types of interstices. Figure 2 illustrates these interstices. The model provides for free movement of electrons between occupied and vacant interstices, but the average electron distribution retains a degree of localization of electron density. Electron correlation is a built-in feature of the model due to (1) the geometry of interstices, (2) the effects of screening of $\bar{e}$ repulsions by ion cores and (3) the spin restrictions based on type of interstice.

This paper will treat the metals of Group I—V and will propose electronic structures for all of them in terms of the metal ion core charge and numbers of electrons in oct and tet interstices. These will be illustrated by electron density diagrams for different crystal planes for representative metals. Metals beyond Group V have localized d-electrons and are discussed separately along with their magnetic properties in Part IV.

1. Interstitial-Electronic Structures of Metals

No attempt will be made to use the interstitial-electron model to predict types of lattice for various metals. The differences in energy between HCP and CCP, *e.g.*, are very small.[2] The model will be used to specify the spatial location of electrons in Group I—V metals, and it will be shown in Part III that such a description of a metal can give considerable insight into the many unusual gradations of metal properties.

In assigning electrons to interstices as discussed above the primary guides will be an assessment of screening of $\bar{e}$ by ion cores in a given structure and the restrictions on electron spin. Whenever unusual features such as lattice distortion or asymmetry in magnetic susceptibility indicate definite electron distributions, these data will be taken into account in assigning electrons to interstices. Since electron pairing in interstices requires considerable energy the minimum number of $(\bar{e})_2$ will be proposed for higher valent metals.

1.1 Alkali Metals. The BCC structure observed for Li, Na, K, Rb, and Cs at ordinary temperatures has 2 M^{n+} per unit cell and the 2 itinerant electrons are expected to occupy tet ring interstices (See Part I). The structure for potassium metal can be written

1) O. Johnson, This Bulletin, **45**, 1599 (1972).

2) W. R. Harrison, "Pseudopotentials in the Theory of Metals," W. A. Benjamin, Inc, N. Y., (1966).

$$|2K^+,\ 2\bar{e}_{tet.\ rings}|BCC.$$

An instantaneous picture of the electron distribution could be occupancy of 2 face tet and 4 edge tet per unit cell. On the average there would be 1/6 occupancy of the interstices by electrons where the interstices are the interlocking rings described in Part 1. To illustrate the electron densities indicated by the model, areas of electron concentration (flat maximum) are shown for different crystal planes on Fig. 1.

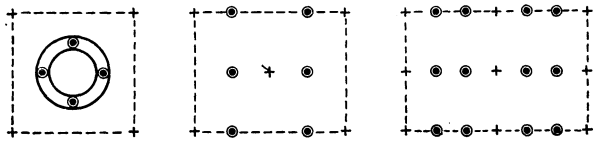

Fig. 1a. Location of interstitial electrons in BCC metals (100, 110, and 111 plane)
(⊙=electron in tetrahedral rings)

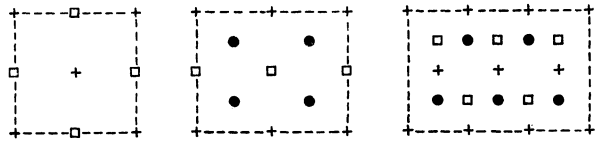

Fig. 1b. Location of interstitial electrons in CCP metals (100, 110, and 111 plane)
(□=oct interstices, ●=tet interstices, +=positive ion cores)

The same structures are expected for Na, Rb, and Cs as given for K. Lithium has certain unusual properties, *e.g.* a higher electronic heat capacity and magnetic susceptibility than Na, and a relatively large lattice displacement. These differences suggest a weaker field of the ion core for Li which might arise from some localization of electron density in one type of interstice or asymmetry of electron density in an interstice.

Both Na and Li form HCP structures at low temperatures. That for Na has a normal c/a ratio and is written with equal $\bar{e}$ distribution in oct and tet interstices:

$$|2Na^+,\ \bar{e}_{oct},\ \bar{e}_{tet}|HCP$$

On the average there is 1/2 occupancy of oct interstices and 1/4 occupancy of tet interstices. The HCP structure of Li has a c/a ratio of 1.563, and this distortion changes 2 tet interstices to a single bipyramidal (BP) interstice. The following structure suggests a greater number of $\bar{e}$ in BP interstices which give greater screening of $\bar{e}$ by ion cores than oct:

$$\left|2Li^+,\ \underset{BP}{\bar{e}_{1+n}},\ \underset{oct}{\bar{e}_{1-n}}\right|HCP$$

the value of n is believed to be small (0.1) since the relative preference for BP is reduced for all $\bar{e}$ over 1.

In view of the small ($1s^2$) ion core for Li^+, unusual properties are not unexpected. They occur as well for Li^+ in solution and for Li compounds and have been interpreted[3] as an especially strong local interaction of Li^+ with cations or solvent molecules. In Li metal, polarization of the $\bar{e}$ cloud could lead to asymmetry in $\bar{e}$ distribution in interstices. Any distortion from optimum $\bar{e}$ distribution would be equivalent to weaker binding forces for Li^+. The general nature of the distortion would be to increase $\bar{e}$ density around the cores. The lattice distortion observed represents the lowest energy arrangement for Li^+ ion cores and the polarized $\bar{e}$ cloud.

1.2 Noble Metals. Although there is a preference for tet occupancy in CCP metals the diamagnetism of Cu, Ag, and Au requires that there be equal numbers of itinerant electrons of each spin. The following structure is proposed for these metals with Cu as example:

$$|4Cu^{11+}(d^{10}),\ 2\bar{e}_{oct},\ 2\bar{e}_{tet}|CCP$$

Placement of electron pairs in tet interstices to satisfy the preference for tet occupancy in CCP is unlikely for a monovalent metal with so many vacant interstices. No properties of copper indicate any special localization. The differences between the alkali and noble metals arise mainly from the larger and more polarizable outer 18-electron shell of Cu, Ag, and Au. The ion core is written above to show the *d*-shell for copper. Because of the poor screening[4] provided by the *d* and *f* electrons the ion core for noble metals has a relatively stronger field than in alkali metals. Itinerant electrons can interpenetrate such ion cores, and the non-rare-gas shell ion core constitutes an exception to the proposed non-penetrability of ion cores. The way electrons are distributed on the (1,1,0) face of a copper unit cell is shown in Fig. 1. This can be considered to show $\bar{e}$ in binding regions as discussed in Part I. The extension of *d*-orbitals into interstitial regions should also be part of such diagrams. This aspect is treated fully in the discussion of magnetic properties in Part IV.

TABLE 1. ELECTRONIC STRUCTURE OF DIVALENT METALS

Be	$\|2Be^{2+},\bar{e}_{1\frac{1}{4}BP}(\bar{e}_2)_{3/4BP},\bar{e}_{1\frac{1}{4}oct}\|$HCP
Mg, Ca,[a] Sr[a]	$\|2M^{2+},2\bar{e}_{oct},2\bar{e}_{tet}\|$HCP
Ca, Sr	$\|4M^{2+},4,\bar{e}_{oct},4\bar{e}_{tet}\|$CCP
Ba	$\|2Ba^{2+},4\bar{e}_{tet\cdot rings}\|$BCC
Zn	$\|2Zn^{2+},1.8\bar{e}_{tet},1.8,\bar{e}_{oct},(\bar{e}_2)_{0.2\,oct}\|$HCP
Cd	$\|2Cd^{2+},1.6\bar{e}_{tet},1.6\bar{e}_{oct},(\bar{e}_2)_{0.4\,oct}\|$HCP

a) Structure at high temperature

1.3 Alkaline Earth Metals, Zinc, and Cadmium. All three lattice types are represented in the alkaline earth metals. As shown in Table 1 an equal distribution in oct and tet interstices is proposed for Ca, Mg, Sr, and Ba in the different lattices. The equal oct and tet preference is quite certain for CCP calcium; it then follows that similar distribution of $\bar{e}$ occurs in HCP and BCC structures since there is very little energy difference between these structures. Beryllium is the unusual metal in the alkaline earth group. Its HCP lattice with c/a of 1.567 has the same kind of distortion as Li in the HCP form. Also, Be is diamagnetic while the other alkaline earth metals have the usual weak paramagnetism of metals. Be has a large positive Hall coefficient,[5] which is discussed in Part III and

3) K. Fajans and O. Johnson, *T. Electrochem. Soc.*, **82**, 273 (1942).

4) O. Johnson, *J. Chem. Educ.*, **47**, 431 (1970).

5) R. J. Weiss, "Solid State Physics for Metallurgists," Pergammon, Oxford, (1963).

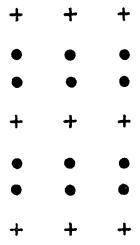

2a. Plane along c-axis

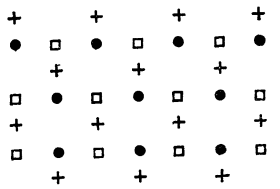

2b. Close-packed layer for HCP ($c/a<1.633$) ●=tet, in plane □=oct, above and below plane

2c. Row of tet interstices in Normal HCP

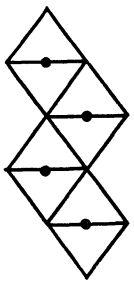

2d. Bipyramidal Interstices in Distorted HCP

2e. Row of oct interstices

Fig. 2. Interstitial electrons in HCP metals. (●=tet interstices, □=oct interstices)

connected with presence of electron pairs in the structure. Thus, a different structure is proposed for Be metal with $(\bar{e}_2)$ in BP interstices (See Fig. 2). This localization of electron density in BP interstices explains the above properties as well as the anisotropy of the diamagnetism. The hardness of Be also reflects localization of electron density.

The localization of $\bar{e}$ in one interstice in Be metal results from the requirement that only 1 unpaired $\bar{e}$ can be in the 2 oct Interstices adjacent to a BP interstice. As with Li the strong polarization of $\bar{e}$ by the $1s^2$ core of Be^{2+} leads to a distorted lattice to satisfy energy requirements. There is anisotropy of the diamagnetic susceptibility of Be with values of -21.4 parallel to c-axis and -7.2 perpendicular to c-axis (at 300°C).[6] This is probably the result of the greater density of Be^{2+} cores and $\bar{e}$ in the parallel direction.

Zinc and Cadmium form HCP structures with strong axial distortion ($c/a=1.856$ and 1.88, respectively). There are no restrictions on spin since there can be an alternation of spins in both oct and tet interstices as in the normal HCP lattice. The electronic structure for Zinc must also reflect the magnetic susceptibility of Zinc which when corrected for the diamagnetism of the core is weakly paramagnetic.[6]

The Zn^{2+} core contains d-electrons and in addition to its high+field this ion core is very deformable compared to rare gas shells (Mg^{2+}, Ca^{2+}) and there will be interpenetration of the $Zn^{12+}(d^{10})$ core by $\bar{e}$. This leads to a different localization or asymmetry of $\bar{e}$ in interstices than observed for Be. It is assumed in the structure written below that there is a small localization as $(\bar{e})_2$ in oct.

$$\left|2Zn^{12+}(d^{10}),\ 1.8\bar{e}_{tet},\ 1.8\bar{e}_{oct},\ (\bar{e}_2)_{\substack{0.2\\oct}}\right|\text{HCP}$$

As with Be the greater diamagnetic susceptibility[6] is observed for Zn in the direction parallel to the axis. In this case it must be the distortion of the ion core in this direction which leads to the small anisotropy. The smaller localization of $\bar{e}$ in tet is compatible with greater extension of d-orbitals along the c-axis.

Cadmium metal must have a very similar structure. The structure proposed below has greater electron localization than for Zn to account for the higher diamagnetic susceptibility of Cd *i.e.* diamagnetic when correction is made for the core diamagnetism.[4]

$$\left|2Cd^{2+},\ 1.6\bar{e}_{tet},\ 1.6\bar{e}_{oct},\ (\bar{e}_2)_{\substack{0.4\\oct}}\right|\text{HCP}$$

The anisotropy[6] of the diamagnetic susceptibility is very high for Cd and has a large decrease with decreasing temperature. This is expected for the more polarizable Cd and also is in keeping with greater localization of $\bar{e}$ in oct. Placement of electrons in unit cells are shown for some of these Group II metals in Fig. 2. Mercury is discussed in section 9 with other non-close packed metals.

1.4 Trivalent Metals. HCP structures are more prevalent for trivalent metals than CCP, and BCC structures are not observed. The CCP structure for Al can be specified rather closely. Because there are more itinerant electrons and because there must be equal numbers of single electrons in oct and tet interstices for balancing of electron spin, there will be electron pairs in all of the trivalent metals. For the CCP structure of Al the pairing is expected for tet interstices. The following structure has the minimum amount of electron pairing:

$$|4Al^{3+},\ 2(\bar{e}_2)_{tet},\ 4\bar{e}_{tet},\ 4\bar{e}_{oct}|\,\text{CCP}$$

This structure has 66% of the electron density in tet interstices. It is also important that the structure leaves some interstices vacant. A smaller fraction of pairs in tet would also require pairing in oct interstices which is not reasonable in CCP lattices. More pairs in tet would lead to some vacant tet interstices which is not reasonable considering the extra energy required for electron pairing. The above structure with 66% of electron density in tet then seems optimum for Al. This will have the same $\bar{e}$ distribution as Cu (Fig. 1). It is of interest that this is a very similar result to that of Harrison[2] who calculated electron density for CCP Al by the method of pseudopotentials. In Fig. 3 which is Harrison's electron density map for Al the tet interstices are indicated. These are regions of slightly greater electron density than the oct regions also indicated in Fig. 3. An estimate of electron density from the contour lines gives 60—70% of the interstitial electrons in the tet interstice region. This can be taken as an independent confirmation of the kind of localization of electrons proposed in the interstitial-electron model. Including $\bar{e}$ around cores, Harrison estimates a small interstitial localization.

Although indium has a tetragonally distorted CCP lattice ($a_0=3.244$, $c_0=4.938$), there is no property

6) W. M. Lomer and W. E. Gardner, *Prog. Metals Science*, **14**, 145 (1969).

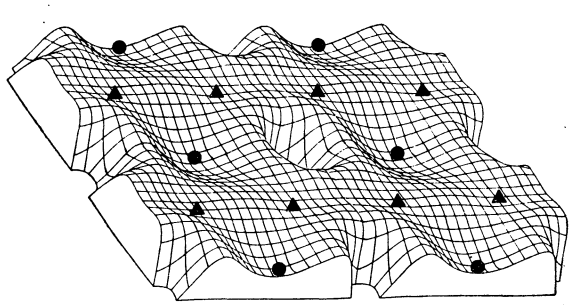

Fig. 3. Relative electron density on a (1, 1, 0) plane in aluminum.
(from W.A. Harrison, "Pseudopotentials in the Theory of Metals," W.A. Benjamin, Inc., New York, 1966)
(▲=ē in tet interstices,
●=ē in oct interstices from interstitial-electrom model.)

which indicates that the structure would differ markedly from that of Al. Since In^{3+} (or $In^{13+}(d^{10})$) has a deformable ion core like Zn, the distortion of the lattice is another example of a means of achieving the lowest energy structure.

The metals Sc and Y have relatively small ion cores ($3s^2$, $3p^6$) and are cations with strong positive field like Be and Li. If is not unexpected that they have HCP lattices with the same distortion ($c/a<1.633$). La is also classed with these metals although it has a more complex layer structure. Tl has an especially strong positive field because of the poor screening by its $4f$ electrons. This apparently puts it with Sc, Y, and La in spite of its deformable character.

The following structure is proposed for the metals Sc, Y, La, and Tl:

$$|2M^{3+}, \bar{e}_{1/2BP}, (\bar{e}_2)_{1\frac{1}{2}BP}, e_{1/2oct}, (\bar{e}_2)_{oct}|HCP$$

This structure has the maximum number of unpaired electrons compatable with spin requirements in this type of HCP lattice. An alternate structure would be:

$$|2M^{3+}, 2\bar{e}_{oct}, 4\bar{e}_{BP}|HCP$$

In this case the occupancy of BP could be considered as 2 ē or as $(\bar{e})_2$. The high value of electronic heat capacity indicates electrons at high energy levels. The observed 30% greater diamagnetic susceptibility for Sc in the direction of the c-axis is expected for this type of lattice distortion. For Tl the anisotropy is even greater. Gallium metal is discussed in section 9.

The rare earth metals are predominantly trivalent and differ from other trivalent metals in having the $4f$ electron shell occupied. Arrott[7] has surveyed the properties of the f-shell containing metals and concluded that with the exception of Eu and Yb, the rare earth metals donate 3 ē to the metal lattice as itinerant electrons. It is because of the unusual stability of the half filled and completely filled f-shell that only 2 ē are itinerant for Eu and Yb. The reduced number of itinerant electrons is shown by greater atomic volume, the BCC structure instead of close-packed, lower MP and lower cohesive energy for Eu and Yb than the other rare earth metals. Kasuya[8] has discussed the differences in properties and structures of the heavy and light rare earth metals.

The interstitial electron structure for Eu and Yb below is proposed to be the same as that of BCC Ba, with difference in properties expected from the very different ion cores in RE

$$|2M^{2+}, 4\bar{e}_{tet.\ rings}|BCC$$

For Pr and Nd which have normal La type HCP structures and for Ce which has HCP at high temperature the following interstitial-electron structure is proposed (similar interstices exist for the La-type lattice):

$$|2M^{3+}, 2\bar{e}_{oct}, 2\bar{e}_{tet}, (\bar{e}_2)_{tet}|HCP$$

alternative structure: $|2M^{3+}, 2\bar{e}_{oct}, 4\bar{e}_{tet}|HCP$

For the heavy Rare Earth Metals (Gd, Tb, Dy, Ho, Er, Tm) which have c/a ratios in the range 1.57—1.59 the following structure (like Sc) is proposed:

$$|2M^{3+}, \bar{e}_{1/2BP}, (\bar{e}_2)_{1\frac{1}{2}BP}, \bar{e}_{1/2oct}, (\bar{e}_2)_{oct}|HCP$$

Variations in ē distribution are anticipated and may be estimated from Hall coefficients or magnetic anisotropy but no attempt will be made to evaluate them at this time.

The CCP structures for Ce and Pr are proposed to be the same as that for Al. The detailed structures of rare earth metals which are ferromagnetic will be discussed in a separate paper.

1.5 Tetravalent Metals. At ordinary temperature the structures for Ti and Zr are HCP with c/a ratios of 1.593 and 1.581 respectively. This distortion leads to oct and bipyramidal interstices and 4 itinerant electrons in 2 interstices would lead to only pairs and complete occupancy. These metals are paramagnetic and have a negative Hall coefficient so there must be unpaired electrons in these metals. Since the distortion is very small for these metals the bipyr (or tet) electrons need not be paired as was suggested also for trivalent metals. The following structure formulates Ti and Zr in this way:

$$|2M^{4+}, 2(\bar{e}_2)_{oct}, 4\bar{e}_{tet}|HCP$$

This electronic structure is also in keeping with the large electronic heat capacity for these metals. The absence of $(\bar{e})_2$ in tet may imply some asymmetry in ē distribution within the tet interstices.

There are BCC structures for Hf and for Ti and Zr at high temperatures. The structure written below with a minimum of electron pairs has 1/3 occupancy of interstices by 2 ē per ring which probably act as electron pairs. Since polymorphic structures do not differ greatly in energy this is an additional reason for considering the HCP structures of Ti and Zr as above with only 1/2 occupancy by electron pairs.

$$|2M^{4+}, 8\bar{e}_{tet.\ rings}|BCC$$

The latter structure shows how the BCC lattice can accomodate more electrons without extensive pairing. This arises because there is equal preference for and equal numbers of the two kinds of interstices (rings around face and edge).

The CCP structures for Pb and Th are formulated as follows:

7) A. Arrott in G. T. Rado, and H. Suhl, "Magnetism," Vol. II B, Acad. Press, N. Y., 1966, p. 339.
8) T. Kasuya, *ibid.*, p. 230.

$$|4M^{4+}, 4(\bar{e}_2)_{tet}, 4\bar{e}_{tet}, 4\bar{e}_{oct}|\,CCP$$

These electronic structure for Pb and Th have 75% of the electron density in tet interstices. This strong localization of $\bar{e}$ density is probably counter-balanced by distortion of the very deformable ion cores which contain both *d* and *f* shells.[4)]

1.6 Pentavalent Metals. V, Nb, and Ta all have the BCC structure and can be formulated as follows with the minimum number of electron pairs (2/3 occupancy):

$$|2M^{5+}, 10e_{tet.\ rings}|\,BCC$$

The possible electronic structures for Bi, As, and Sb are discussed in the following section along with other metals which do not have close packed structures.

2. Interstitial-Electron Structures for Non-close-packed Metals

Mercury is a liquid at room temperature, and gallium melts just above room temperature. Solid mercury has a rhombohedral structure and the CN of Hg^{2+} is 6. Compared to a simple cubic lattice the interaxial angle is 70° 1/2. *Gallium* has an orthorhombic structure with two identical axes of its pseudotetragonal unit. There are 8 atoms per unit cell, a_0 and b_0 (1.5107) and c_0 (7.6448). There are 2 neighbours at 2.71, 2 at 2.80, and 1 at 2.44 Å. Bent[9)] has pointed out that gallium sulfide has 2 Ga-Ga at short distance and 6Ga-Ga larger distances with the suggestion of electrons pairs in gallium metal where anions are placed in the sulfide. The interstitial electron model cannot specify the location of electrons in Ga and Hg. There are likely to be $-Ga^{3+}\ (\bar{e})_2\ Ga-^{3+}$ units in the structure along with single electrons in interstitial positions. The combination of long range and short range order probably accounts for the liquid state at low temperatures.

White tin is tetragonal with a_0 of 5.8197 and c_0 of 3.1748. Each ion core is surrounded by a distorted tetrahedron of Sn neighbours at 3.02 Å with 2 more Sn in the axial positions at 3.17 Å. Although white tin deviates from a close packed structure the interstices are related to those of CCP, and the structure proposed is similar to that of lead:

$$|4Sn^{4+}, 4(\bar{e}_2)_{tet}, 4\bar{e}_{tet}, 4\bar{e}_{oct}|\,Tetrag.$$

Some asymmetry in the $\bar{e}$ distribution within oct and within tet interstices is expected from the lattice distortion. The slightly greater diamagnetic susceptibility in the direction perpendicular to the *c*-axis[10)] is compatable with ion core distortion and greater core numbers in that direction.

Gray tin has the diamond structure and is non-metallic. It will be mentioned to illustrate the difference in chemical binding. The distance of 2.80 Å between Sn^{4+} is about 10% less than for white tin. Electron pairs $(\bar{e}_2)$ between all Sn^{4+} tetrahedrally arranged are expected as in Ge or diamond as written below:

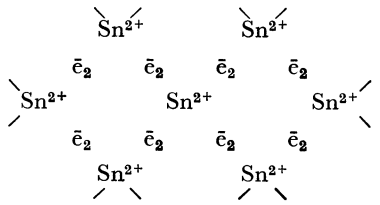

Bismuth crystallizes in a puckered layer lattice with a CN of 3. It is unusual in that it has the highest diamagnetic susceptibility of all the metals.[10)] In the tetragonal Bi_2O_3 lattice each Bi^{3+} has 6 O^{2-} neighbours (related to Mn_2O_3 lattice). In bismuth metal there is the counterpart of the octahedral hole in the puckered layer and if all the octahedral interstices are filled there remains an $(\bar{e})_2$ per 2 Bi^{3+}. This may well be within the layers as follows:

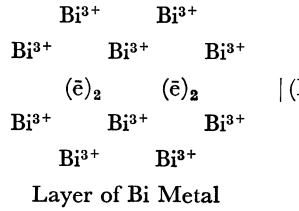

Layer of Bi Metal

$|(Bi_2^{3+}(\bar{e})_2), 2(\bar{e})_2$ in oct. inter.|

Structure of Bi Metal

The filled octahedral interstices would explain the low electric conductivity and the $(\bar{e})_2$ associated with the layers can account for the very large diamagnetic susceptibility as well as the anisotropy of the diamagnetism.

The related elements As and Sb depart further from metallic behavior. The layer spacing increases from Bi to Sb to As and thus they deviate further than Bi from close-packed structures.

3. Conclusions

Electronic structures have been proposed for all the Group I—V metals. In most cases a precise electronic structure could be given in terms of $\bar{e}$ occupancy of interstices. In a few cases alternate structures or a range of possible occupancies was given. The areas of electron localization could also be indicated for various crystal faces in terms of the electron model. These represent electrons in the binding areas of the interstices in a metal and should be useful in interpreting both chemical and physical properties of metals.

The relation of $\bar{e}$ and $(\bar{e}_2)$ in metal interstices to a number of properties (*e.g.* Hall coefficient, magnetic susceptibility) has been used as a guide in formulating interstitial-electronic structures in some cases. It has been possible to correlate metal properties with the interstitial-electron distribution, and this is presented in detail in Part III. It may be possible to further refine the structures given in this paper on the basis of experimental data on metal properties.

The interstitial-electron structures proposed on the basis of simple rules for occupancy of interstices show the greatest localization of $\bar{e}$ density in just those HCP and CCP structures which are distorted from normal close packing. Ion cores with strong positive fields (*e.g.*, Li^+, Be^{2+}) are expected to polarize the itinerant $\bar{e}$ cloud. Ions containing *d* and *f* electrons[4)] are expected also to have strong positive fields but these

9) H. Bent, *J. Chem. Educ.*, **45**, 768 (1968); **42**, 348 (1965).
10) L. F. Bates, "Modern Magnetism," Cambridge Univ. Press, Cambridge, 3rd Ed, (1951).

non-rare gas shells are deformable and will be penetrated by itinerant electrons. These polarizing effects of and on itinerant electrons are held to be the cause of the lattice distortion. These polarization and interpenetration effects are less important when there are few $\bar{e}$ and when there are predominantly ($\bar{e}_2$) in the interstices and thus predominate for divalent and trivalent metals.